Ullsperger M, von Cramon DY (2001) Subprocesses of performance monitoring: a dissociation of error processing and response competition revealed by event-related fMRI and ERPs. Neuroimage 14:1387-401.

Van 't Ent D, Apkarian P (1999) Motoric response inhibition in finger movement and saccadic eye movement: a comparative study. Clin Neurophysiol 110:1058-72.

Van 't Ent D (2002) Perceptual and motor contributions to performance and ERP components after incorrect motor activation in a flanker reaction task. Clin Neurophysiol 113:270-83.

Van Veen V, Carter CS (2002) The timing of action-monitoring processes in the anterior cingulate cortex. J Cogn Neurosci 14:593-602.

Vidal F, Hasbroucq T, Grapperon J, Bonnet M (2000) Is the 'error negativity' specific to errors? Biol Psychol 51:109-28.

West R, Alain C (1999) Event-related neural activity associated with the Stroop task. Brain Res Cogn Brain Res 8:157-64.

Yordanova J, Falkenstein M, Hohnsbein J, Kolev V (this issue) Parallel Systems of Error Processing in the Brain.

Are all medial frontal negativities created equal? Toward a richer empirical basis for theories of action monitoring

William J. Gehring and Adrian R. Willoughby
University of Michigan

Theories and empirical studies concerned with the action monitoring functions of the medial frontal cortex have generally assumed that numerous medial frontal negativities--such as the error-related negativity (ERN/Ne), N2, and the negativity elicited by error feedback and monetary losses--all reflect the activity of a common underlying neural generator. Several reports have asserted that the ERN and the feedback negativity both reflect the same underlying neural activity, and an influential model postulates that both components represent activity generated when the anterior cingulate cortex receives an error signal indicating that an event is "worse than expected." In this paper, we use time-frequency analysis based on the continuous wavelet transform to test the proposal that the ERN and the feedback-related medial frontal negativity are equivalent. We find that the two components are not identical in their scalp distribution, indicating that a single, common source cannot be the only source generating the two components.

Introduction

A recent trend in studies of the action monitoring functions of the medial frontal cortex has been to focus on scalp potentials that resemble the ERN/Ne but that occur following events other than error responses. In this chapter, we call this broad class of ERP components "medial frontal negativities" (MFNs), referring to the medial frontal scalp distribution that they share. The MFNs comprise a growing list of potentials, including the ERN/Ne elicited by error responses in reaction time tasks (Falkenstein et al., 1991; Gehring et al., 1993), the N2-like potentials elicited by error feedback stimuli (Miltner et al., 1997; Holroyd and Coles, 2002; Ruchsow et al., 2002) and by monetary losses in simple gambling tasks (Gehring and Willoughby, 2002), the variety of N2-like potentials elicited in situations of response conflict or response inhibition (Gehring et al.,1992; Kopp et al., 1996; Falkenstein et al., 1999), and even the classic oddball N2 (Nieuwenhuis et al., 2003). This class of ERP components also includes some that are less well-understood, such as the small negativity that sometimes follows the ERN (Fiehler and Ullsperger, 2003), the ERN-like potential that sometimes accompanies correct responses (Vidal et al., 2000; Gehring and Knight, 2001), and midline frontal theta oscillations (Luu and Tucker, 2001).

An emerging, unresolved issue is, therefore, which electrophysiological phenomena should be explained by a theory of the ERN/Ne and which should not. Two computational models dominate current theorizing. One of these, the conflict-detection model (Carter et al., 1998; Botvinick et al., 2001) was developed to explain the ERN and hemodynamic responses in neuroimaging studies of

the anterior cingulate cortex (Carter et al., 1998). The empirical phenomena it explains have grown to include the N2 elicited when attributes of a stimulus call for conflicting responses, the N2 elicited by no-go stimuli, and the oddball N2 (Nieuwenhuis et al., 2003). However, the proponents of the conflict-detection model have remained noncommittal concerning the relevance of conflict-detection to components elicited by error feedback and monetary losses (Botvinick et al., 2001). The reinforcement-learning model (Holroyd and Coles, 2002), in contrast, seeks to explain both the ERN and the negativities elicited by error feedback and monetary losses, but it excludes the N2 (Holroyd and Yeung, 2003). Each model has yet to specify the relationship between its predictions and midline frontal theta.

Comparing the explanatory abilities of models is difficult when they disagree on which core findings they must explain. Without principled, a priori reasons for including or excluding certain MFNs, the models possess the undesirable property of being free to redefine the relevant phenomena in a post hoc fashion in response to new evidence. Although this is certainly a problem for computational models, it is compounded in ERP research, where a fundamental, lingering problem is that an ERP phenomenon recorded in one experimental paradigm may be morphologically quite similar to one recorded in some other paradigm yet be generated by a different configuration of cortical sources (Allison, Wood and McCarthy, 1986).

One step toward stronger models, then, is to constrain theorizing by developing finer-grained characterizations of the ERPs themselves. The present study represents one such step. Here, we compared the response-related ERN and the feedback-related negativity recorded from the same group of subjects. To characterize the potentials in a more detailed manner, we used time-frequency analysis based on the Morlet wavelet transform to separate activity associated with the ERN and feedback-related MFN from overlapping, lower-frequency components. Our use of wavelet analysis was motivated in part by the proposal that the ERN reflects activity in the theta (4-7 Hz) frequency range (Luu and Tucker, 2001).

Because of the limited space we can only touch on the details of wavelet analysis; we refer the reader to useful tutorials by Farge (1992) and Torrence and Compo (1998). The continuous wavelet transform computes the convolution of the ERP waveform with several contracted and expanded versions of a canonical function known as the mother wavelet. There are numerous mother wavelets from which to choose. In the case of the Morlet wavelet, the one we use here, the mother wavelet is complex sine wave modulated by a Gaussian envelope. There is a straightforward analytic relationship between the scale of the Morlet wavelet and the frequency to which it is maximally sensitive (Torrence and Compo, 1998). As a result, the multiple contracted and expanded "daughter" wavelets are high- and low-frequency versions of the mother wavelet. One can plot the wavelet coefficients (i.e., the correlations of the ERP and the wavelet) at the different frequencies as a time-frequency surface, which depicts at each point in time and frequency the correlation between the ERP waveform and the daughter wavelet at that point (Farge, 1992; Torrence and Compo, 1998). The practical advantage of this method for analyzing ERPs is that it allows one to extract activity in a particular frequency band (for example, the ERN-like activity at 4-7 Hz) from slower, overlapping activity (such as the P3e), reducing the possibility that overlapping components will contaminate measures of the ERP of interest.

The goal of our experiment was thus to compare the spatial and time-frequency characteristics of the ERN and feedback-related MFN. Participants performed a standard Eriksen flanker task (cf. Gehring et al., 1993) and a simple gambling task based on the one reported in Gehring and Willoughby (2002). We used the wavelet transform to compute a time-frequency surface for each electrode in each condition, depicting power relative to a pre-stimulus baseline (see Makeig, 1993). We identified the regions on the time-frequency surface associated with the ERN and the feedback-related MFN, and then we compared the scalp topographies of the power within these regions. Topographic analysis cannot show that two components are the same, because different neural generators can cause topographically identical phenomena. It can, however, show two components

to be different: a difference in scalp topographies implies that the underlying configuration of neural generators must be different (McCarthy and Wood, 1985; Ruchkin et al., 1999).

Methods

6 male and 10 female participants (mean age 21.7 years, range 18.6 – 25.6) participated. The study was divided into two halves, one being the flanker task and the other being the gambling task. The order of the two tasks, the assignment of stimulus to response hand in the flanker task, and the assignment of color (red or green) to gains and losses were counterbalanced across participants. Participants were paid $8 an hour and had the opportunity to win bonus money as described below. The EEG was recorded using an Easycap (http://www.easycap.de) on which sintered Ag/AgCl electrodes were placed at Nz, Fp1, Fp2, AFz, F7, F3, Fz, F4, F8, FT7, FC3, FCZ, FC4, FT8, T7, C3, Cz, C4, T8, FP7, CP3, CPz, CP4, TP8, P9, P7, P3, Pz, P4, P8, P10, O1, Oz, O2, Iz, and the right mastoid (American Electroencephalographic Society, 1991). EEG data were recorded with a left mastoid reference and forehead ground. An average mastoid reference was derived off-line. The electrooculogram (EOG) was recorded from electrodes placed above and below the left eye and external to the outer canthus of each eye. Impedances were kept below 10 KOhm. EEG and EOG were recorded with SYNAMPS amplifiers (Neuroscan, Inc.) from .01 to 100 Hz (half-amplitude cutoffs). Data were digitized at 500 Hz. EEG and EOG out-of-scale and flat-line artifacts were rejected, and ocular artifacts were corrected using the procedure outlined in Gratton, Coles, and Donchin (1983). For Figure 1, the waveforms were filtered with a 9 point Chebyshev Type II low-pass digital filter, half-amplitude cutoff at approximately 12 Hz. The baseline in that figure is 100 ms pre-response for the flanker task and 100 ms pre-stimulus for the gambling task.

Morlet wavelet analysis was performed using software provided by C. Torrence and G. Compo, available at http://paos.colorado.edu/research/wavelets/. The wavelet analysis used the average waveform for each subject in each condition to derive a time-frequency surface. Then, the mean power (in decibels) in the 300 ms pre-stimulus baseline was subtracted from the mean power across the whole epoch (yielding the event-related spectral perturbation; Makeig, 1993). The pre-stimulus baseline was used for response-locked data to avoid contamination from stimulus-related processing and because of the apparent onset of ERN-like activity prior to the response. Thus the values represented in the time-frequency and topographic plots reflect the change in power in decibels relative to a pre-stimulus baseline.

In the Eriksen flanker task, participants responded to the central letter of a five-letter stimulus array (HHHHH, SSHSS, SSSSS, or HHSHH, duration 100 ms) by pressing one button (on a Neuroscan STIM response pad) with the index finger of one hand if the central letter was an "H" and with the index finger of the other hand if the central letter was an "S." At a viewing distance of 62 cm, the letter string subtended approximately 4.7 degrees of visual angle. A warning symbol ("#"), presented for 100 ms, preceded the letter array by 500 ms and followed the previous letter array by 2 s. A fixation point ("+") was placed 1 degree below the center of the letter array and was visible throughout the block of trials. Participants completed 11 blocks of 80 trials. Prior to each odd-numbered block, participants received an allotment of $2.00. Errors were penalized by a loss of 25 cents, and in each block responses faster than the participant's best mean reaction time from previous blocks were rewarded with five cents.

In the simple gambling task (see Gehring and Willoughby, 2002), participants viewed two empty squares, which together at a viewing distance of 62 cm subtended 3.2 degrees of visual angle. After one second, the numeral 5 appeared in one square and the numeral 25 appeared in the other. Participants chose either the left or the right square by pressing the corresponding button. One second after the response, the color behind the numerals within each square changed color. The feedback stimulus remained on the screen for three seconds and was then replaced by the two empty squares, initiating a new trial. After the response, if the chosen square turned green (red for half of the subjects), then the amount indicated by the numeral (in U.S. cents) was added to the total amount awarded to the participant at the end of a block of trials. If the chosen stimulus turned red (green), then the amount indicated was subtracted from the total. The square that the participant

16

did not choose changed color with the chosen square. As a result, participants not only discovered their gain or loss but they also discovered what they would have gained or lost had they chosen the other square. The color appearing in each square was determined randomly, so the monetary value in the unchosen square always differed from the chosen square in value and could differ in valence. Participants completed 16 blocks of 32 trials. For each set of 4 blocks, participants were given an allotment of $2.50; bonuses were added to or subtracted from that amount and the total at the end of each set of 4 blocks was added to or subtracted from the total bonus awarded to the participant at the end of the experiment.

Results

In the flanker task, responses were slower and less accurate on incongruent trials (396 ms, 92.6% correct) than on congruent trials (364 ms, 97.9% correct; reaction time: F (1, 15) = 82.77, $p <$ .000001, MSE = .0001; proportion correct, $\underline{F}$ (1, 15) = 31.15, p = .000052, MSE = .00072).
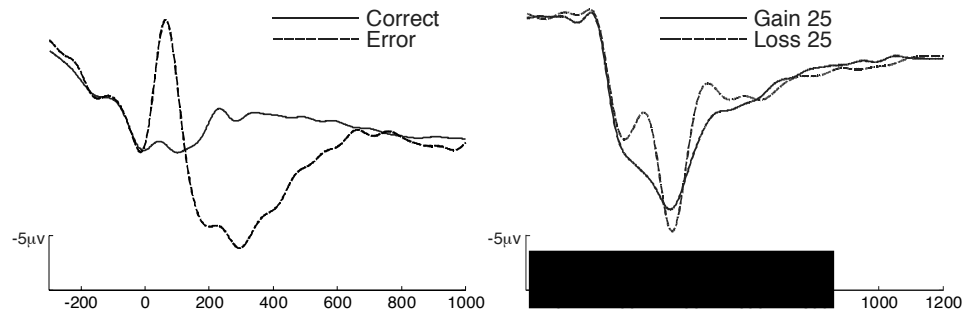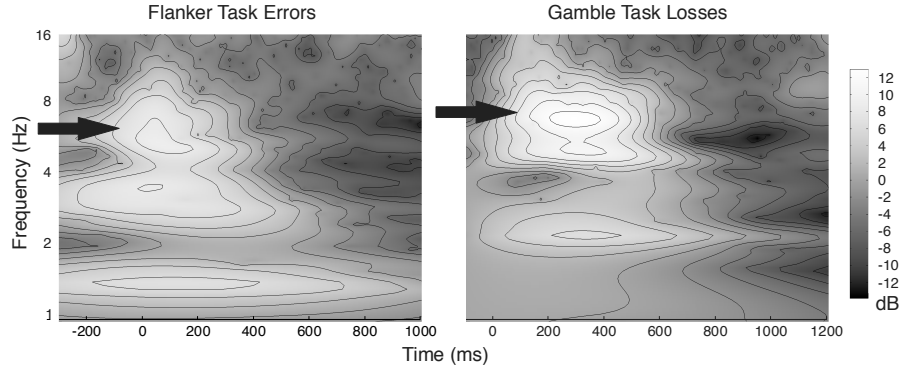

Figure 1.
Response-locked error-related negativity from the flanker task at the FCz electrode (left) and stimulus-locked feedback-related negativity from the gambling task at the Fz electrode (right). Time zero is the moment of response onset in the flanker task and the moment of stimulus onset in the gamble task.

ERP waveforms at FCz for error and correct trials from the Flanker task, averaged across subjects, are shown in the left panel of Figure 1. Waveforms at Fz for gain and loss trials from the gambling task are shown in the right panel. (We show different electrodes because of the topographic differences discussed below.) To quantify the ERN and feedback-related MFN activity, we computed Morlet wavelet transforms separately for each average waveform, from each condition at each electrode. Wavelet transforms were computed separately for each subject. Figure 2 depicts the surface created by the Morlet wavelet transforms of the error and loss waveforms, averaged across subjects. A clear burst of theta-frequency activity occurs at the time of the ERN and at the time of the feedback-related MFN. The time-frequency surfaces also demonstrate the ability of the wavelet analysis to separate the theta-frequency activity from temporally overlapping, lower-frequency components.

To quantify the theta-frequency activity, we computed for each subject the mean power within a 4-7 Hz frequency band relative to a 300 ms pre-stimulus baseline. The measurement window for the flanker task was 0-100 ms following the response, and for the gamble task it was 200-300 ms following the feedback stimulus. Figure 3 shows the scalp topography of the mean of these power measures for error trials and for loss trials. Topographic maps showing the error-correct and loss-gain differences in power were virtually identical to those shown in the figure.

Interactions of condition and valence with one of the electrode factors thus indicate a difference in the pattern of scalp topography between the gamble and flanker tasks. A significant condition x valence x caudality interaction (F (4, 60) = 9.40, p = .0014, ε = .42, MSE = .077) showed that the distribution of the MFN was more anterior in the gambling (feedback-related MFN) task than in the flanker (ERN) task. A significant four-way interaction (F (16, 240) = 4.34, p = .00044, ε = .41,

17

MSE = .012) was consistent with the pattern begin more right lateralized at frontal sites for the

feedback-related MFN than for the ERN (see Figure 3).

Figure 2.
Time-frequency surfaces computed with the Morlet wavelet transform. The arrow indicates the time-frequency component corresponding to the error-related negativity at FCz (left) and the feedback-related negativity at Fz (right). Time zero is the moment of response (left) and the moment of stimulus onset (right). The color scale represents change in power relative to a 300 ms pre-stimulus baseline, in decibels.
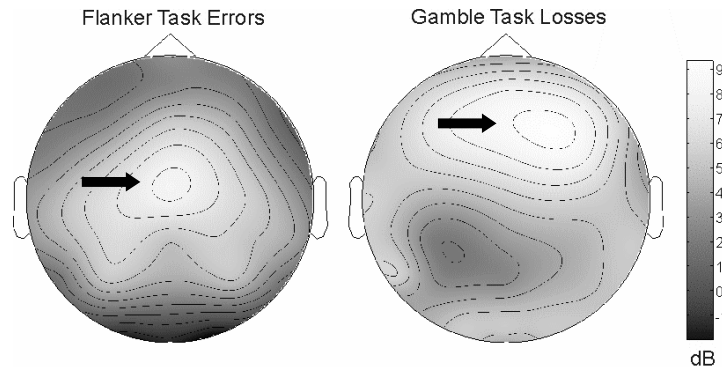

Figure 3.
Scalp topography of 4-7 Hz activity following errors in the flanker task (left) and following losses in the gambling task (right). Values are shown as the mean change in power (dB) relative to a 300 ms pre-stimulus baseline, derived from the Morlet wavelet transform. Arrows indicate the region of maximal activity associated with the error-related negativity (left) and feedback-related negativity (right).

Discussion

The ERN and the feedback-related MFN showed very similar time-frequency characteristics, with both consisting of bursts of activity in the 4-7 Hz frequency range. The scalp topographies of the two components, however, reveal that they are not identical phenomena. The feedback-related MFN is somewhat more right lateralized and anterior in its scalp distribution than is the ERN. For such a difference to occur the configuration of underlying generators cannot be the same. This is not to say that the two components are necessarily completely distinct. It is quite plausible that the two phenomena share one or more neural generators in common; nevertheless, there must be some activity that is not shared. There are two possibilities that could explain the observed pattern of topographic activity: one is that the two phenomena arise from entirely distinct neural generators, the other is that they share some activity but that there is also some distinct activity contributing to one or both components. Perhaps, for example, a single neural generator causing the ERN is active in both cases, with an additional right-hemisphere prefrontal contribution in the case of the

feedback-related MFN. Future studies combining wavelet analysis with source localization techniques may prove useful in clarifying the reasons for the topographic difference observed here. Although our results indicate that the ERN and the feedback-related MFN are not identical, it is still an open question whether the conflict-detection and reinforcement-learning theories of the ERN must also accommodate findings from studies of the feedback negativities. Some or all of the generators of the ERN may be active when the feedback-related MFN is recorded, and vice versa. Our study indicates, then, that with multiple intracranial sources contributing to one or both of the scalp negativities, it is important for studies of these phenomena to characterize fully and report the scalp topography of their ERP effects. Our results also suggest that it is possible to develop richer empirical criteria for determining which ERP phenomena a theory must explain and which it can exclude. By considering time-frequency characteristics, these criteria can augment the more traditional defining criteria of an ERP component, such as latency, polarity, scalp distribution, and sensitivity to experimental condition (Donchin, Ritter, and McCallum, 1978).

Our use of the Morlet wavelet transform as a means of extracting the ERN and feedback MFN from the other, overlapping ERPs was partly motivated by the proposal that the ERN represents part of an oscillation in the theta (4-7 Hz) frequency range (Luu and Tucker, 2001; Luu et al., 2003). Such a proposal is consistent with the ERN-like peaks that often follow the ERN and other MFNs (such as the one that is apparent at around 500 ms in the loss waveform in Figure 1). Nevertheless, finding a region of activity in the 4-7 Hz range on the time-frequency surface does not imply that the activity is oscillatory. The Morlet wavelet is itself oscillatory, and when it is convolved with a single peak in the 4-7 Hz range, the wavelet transform will produce a temporally-extended pattern in the time-frequency surface. Other mother wavelets may be more helpful in distinguishing oscillatory components from single, discrete peaks. The Marr wavelet (second derivative of a Gaussian), for example, produces a time-frequency amplitude plot that shows distinct peaks and valleys corresponding to the peaks in the waveform (although its frequency resolution is not as good as the Morlet wavelet, see Torrence and Compo, 1998). Following the logic used by Yeung et al. (submitted) in their examination of digital filters, we compared a time-frequency surface generated by convolving a Marr wavelet with a single ERP peak with another generated when the wavelet was convolved with a true oscillation. The time-frequency surface resulting from a single peak appeared oscillatory but had a more "flame-like" appearance, with more activity occurring below the frequency of the signal, than did the surface resulting from the oscillatory potential. It may be possible to use the wavelet transform to develop analytic techniques that distinguish oscillatory and non-oscillatory phenomena.

Inspection of the time-frequency surfaces in Figure 2 raises some issues that future work of this type will need to address. First, the time-frequency surfaces were computed from the average waveforms and are thus sensitive to electrophysiological activity that is phase-aligned to the stimulus or response. Future work will benefit from the analysis of single-trial wavelet transforms, which are sensitive to activity that is not phase-aligned to external events. Second, time-frequency components can overlap, and the ability of the wavelet transform to distinguish them will be limited when the components that overlap in time are close in frequency, or those that overlap in frequency are close together in time. In a step toward solving this problem, Bernat, Williams, and Gehring (submitted) have described a method for using principal components analysis to extract distinct time-frequency components from a time-frequency surface. Their technique was developed using time-frequency distributions (a different method for time-frequency analysis), but it could in principle be applied to wavelet analyses. This and similar techniques will be needed in future time-frequency analyses of the medial frontal negativities.

Acknowledgements

References

Allison T, Wood CC, McCarthy G (1986) The central nervous system. In: Psychophysiology: Systems, processes, and applications (Coles MGH, Donchin E, Porges EW, eds), pp5-25. New York: The Guilford Press.

American Electroencephalographic Society (1991) American Electroencephalographic Society Guidelines for Standard Electrode Position Nomenclature. J Clin Neurophys 8:200-202.

Bernat E, Williams WJ, Gehring WJ (submitted) Decomposing ERP time-frequency energy using PCA. Manuscript submitted for publication.

Botvinick MM, Braver TS, Barch DM, Carter CS, Cohen JD (2001) Conflict monitoring and cognitive control. Psychol Rev 108(3):624-652.

Carter CS, Braver TS, Barch DM, Botvinick MM, Noll D, Cohen JD (1998) Anterior cingulate cortex, error detection, and the online monitoring of performance. Science 280(5364):747-749.

Donchin E, Ritter W, McCallum, C (1978) Cognitive psychophysiology: The endogenous components of the ERP. In: Brain event-related potentials in man. (Callaway E, Tueting P, Koslow S, eds.), pp349-441. New York: Academic Press

Falkenstein M, Hohnsbein J, Hoormann J, Blanke L (1991) Effects of crossmodal divided attention on late ERP components: II. Error processing in choice reaction tasks. Electroencephalogr Clin Neurophysiol 78(6):447-455.

Falkenstein M, Hoormann J, Hohnsbein J (1999) ERP components in Go/Nogo tasks and their relation to inhibition. Acta Psychol 101(2-3):267-291.

Farge M (1992) Wavelet transforms and their applications to turbulence. Ann Rev Fluid Mech 24:395-457.

Fiehler K, Ullsperger, M (2003) Error correction: time course and localization. Talk presented at the conference Errors, Conflicts, and the Brain. July 3-5 2003, Dortmund, Germany.

Gehring WJ, Gratton G, Coles MGH, Donchin E (1992) Probability effects on stimulus evaluation and response processes. J Exp Psychol Hum Percept Perform 18(1):198-216.

Gehring WJ, Goss B, Coles MGH, Meyer DE, Donchin E (1993) A neural system for error detection and compensation. Psychol Sci 4(6):385-390.

Gehring WJ, Knight RT (2000) Prefrontal-cingulate interactions in action monitoring. Nat Neurosci 3:516-520.

Gehring WJ, Willoughby AR (2002) The medial frontal cortex and the rapid processing of monetary gains and losses. Science 295(5563):2279-2282.

Gratton G, Coles MGH, Donchin E (1983) A new method for off-line removal of ocular artifact. Electroencephalogr Clin Neurophysiol 55(4):468-484.

Holroyd CB, Coles MGH (2002) The neural basis of human error processing: Reinforcement learning, dopamine, and the error-related negativity. Psychol Rev 109(4):679-709.

Holroyd CB, Yeung N (2003) Alcohol and error processing. Trends Neurosci 26(8):402-404.

Kopp B, Mattler U, Goertz R, Rist F (1996) N2, P3 and the lateralized readiness potential in a nogo task involving selective response priming. Electroencephalogr Clin Neurophysiol 99(1):19-27.

Luu P, Tucker DM (2001) Regulating action: Alternating activation of midline frontal and motor cortical networks. Clin Neurophysiol 112(7):1295-1306.

Luu P, Tucker DM, Derryberry D, Reed M, Poulsen C (2003) Electrophysiological responses to errors and feedback in the process of action regulation. Psychol Sci 14(1):47-53.

Makeig, S (1993) Auditory event-related dynamics of the EEG spectrum and effects of exposure to tones. Electroencephalogr Clin Neurophysiol 86(4):283-293.

McCarthy G, Wood CC (1985) Scalp distributions of event-related potentials: An ambiguity associated with analysis of variance models. Electroencephalog Clin Neurophysiol 62:203–208.

Miltner WHR, Braun CH, Coles MGH (1997) Event-related brain potentials following incorrect feedback in a time-estimation task: Evidence for a "generic" neural system for error detection. J Cogn Neurosci 9(6):788-798.

Nieuwenhuis S, Yeung N, Van den Wildenberg W, Ridderinkhof KR (2003) Electrophysiological correlates of anterior cingulate function in a go/no-go task: Effects of response conflict and trial type frequency. Cogn Affective Behav Neurosci 3(1):17-26.

Ruchkin DS, Johnson Jr R, Friedman D (1999) Scaling is necessary when making comparisons between shapes of event-related potential topographies: A reply to Haig et al. Psychophysiology 36:832-834.

Ruchsow M, Grothe J, Spitzer M, Keifer M (2002) Human anterior cingulate cortex is activated by negative feedback: evidence from event-related potentials in a guessing task. Neurosci Lett 325(3):203-206.

Torrence C, Compo GP (1998) A practical guide to wavelet analysis. Bull Am Meteor Soc 79(1):61-78.

Vidal F, Hasbroucq T, Grapperon J, Bonnet M (2000) Is the 'error negativity' specific to errors? Biol Psychol 51(2-3):109-128.

Yeung N, Bogacz R, Holroyd CB, Cohen JD (submitted) Detection of synchronized oscillations in the electroencephalogram: an evaluation of methods. Manuscript submitted for publication.